Low Voltage Induced Reversible Magnetoelectric Coupling in Fe_3O_4 Thin Films for Voltage Tunable Spintronic Devices

Le Zhang[1, 2], Weixiao Hou[1], Guohua Dong[1], Ziyao Zhou[1*], Shishun Zhao[1], Zhongqiang Hu[1], Wei Ren[1*], Mingfeng Chen[3], Ce-Wen Nan[3], Jing Ma[3], Hua Zhou[4], Wei Chen[2, 5], Zuo-Guang Ye[6, 1], Zhuang-De Jiang[7], Ming Liu[1*]

1. Electronic Materials Research Laboratory, Key Laboratory of the Ministry of Education & International Center for Dielectric Research, Xi'an Jiaotong University, Xi'an 710049, Shaanxi, China
2. Institute for Molecular Engineering and Materials Science Division, Argonne National Laboratory, Lemont, Illinois 60439, United States
3. Department of Materials Science and Engineering, State Key Lab of New Ceramics and Fine Processing, Tsinghua University, Beijing 100084, China
4. Advanced Photon Source, Argonne National Laboratory, Lemont, Illinois 60439, United States
5. Institute for Molecular Engineering, the University of Chicago, Chicago, Illinois 60637, United States
6. Department of Chemistry and 4D LABS, Simon Fraser University, Burnaby, British Columbia V5A 1S6, Canada
7. State Key Laboratory for Manufacturing Systems Engineering, Xi'an Jiaotong University, Xi'an 710049, Shaanxi, China

1. XRD and HRTEM images

There are no other reflections in the Figure S1a could be seen in the whole range except the (200) and (400) peaks of the MgO substrate and (800) peak of Fe_3O_4, which indicates high-quality epitaxial growth of Fe_3O_4 on MgO substrates. High resolution transmission electron microscopy (HRTEM) images with different scale showing sharp interface between the Fe_3O_4 films and the MgO substrate are shown in b-e..

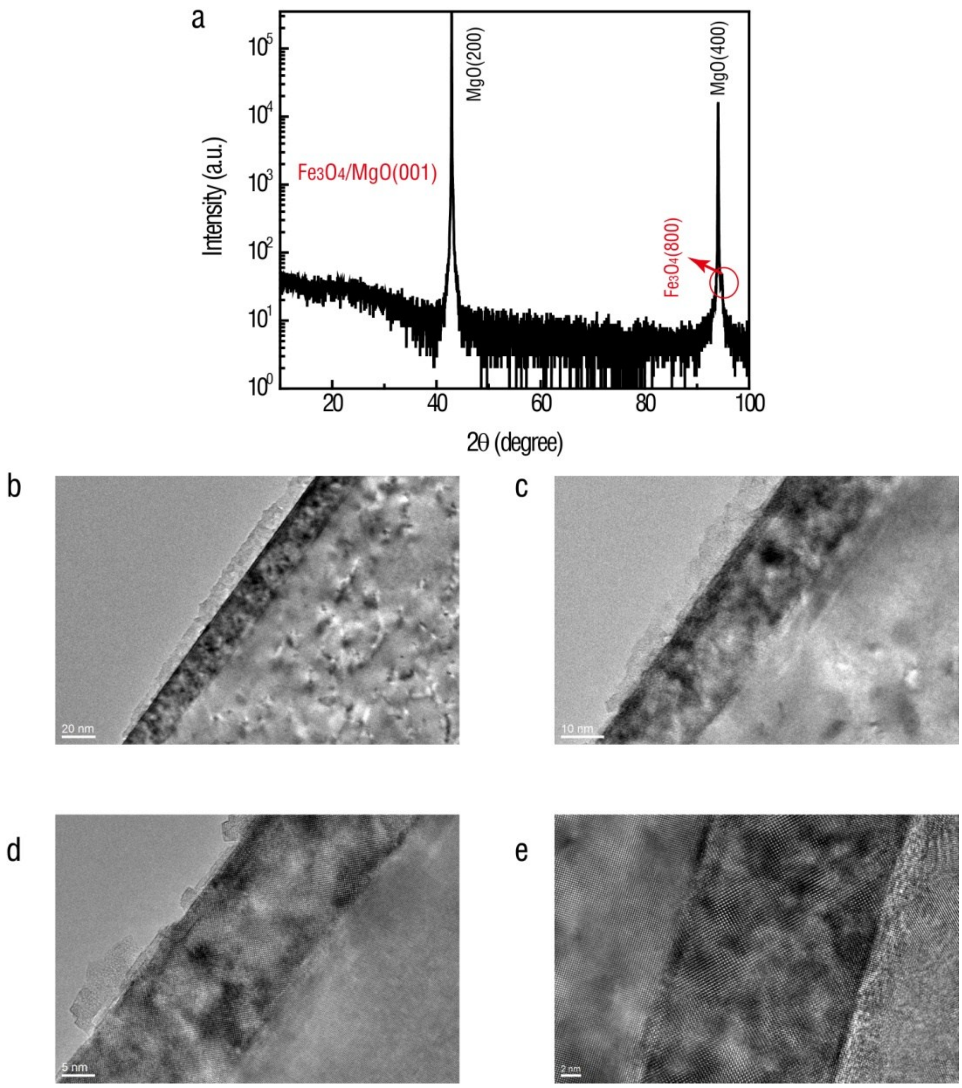

Figure S1(a) X-ray diffraction patterns of the Fe_3O_4/MgO heterostructure. (b-e) Different scale HRTEM images at the interface

2. Out-of-plane VSM curves as a function of gating voltage.

Due to the VSM measurement take place in open environment, it is impossible to keep the same N_2 atmosphere as the EPR test in a closed chamber. It can be seen from the inset in Figure S2 that the coercive field almost keeps constant and the saturation magnetization shows random variations. This is because that in air condition the charge doping and generation of oxygen vacancy especial the latter is different in N_2 condition.

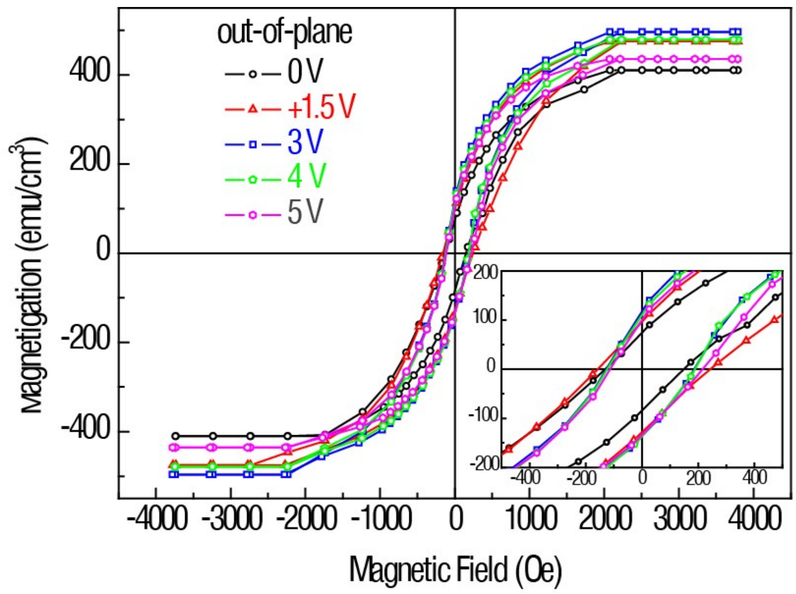

Figure S2 Out-of-plane of *in*-situ VSM test of the Au/[DEME]$^+$[TFSI]$^-$/Fe_3O_4/MgO heterostructure at different V_g. The inset shows the local image near the zero magnetic field

3. Angular dependence of H_r results

H_r increased as a function of V_g (angle<60^o) while the H_r decreased for angle>60^o. It was found that the magnetic easy axis is in the film plane (in-plane) and the hard axis is perpendicular to the film (out-of-plane). The maximum H_r shift was obtained along out-of-plane direction with 280 Oe tunability. Since the greatest tunability was obtained in this direction, the following reversible teat was performed along out-of-plane.

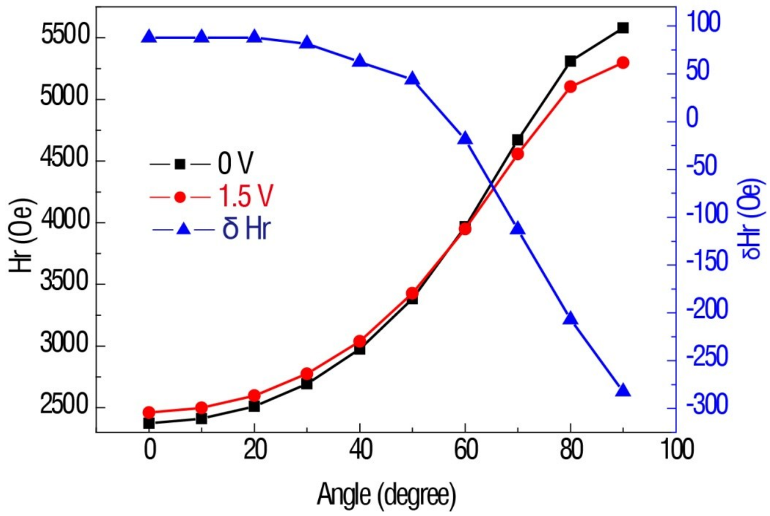

Figure S3 Angular dependence of H_r under 0 V (black square line) and 1.5 V (red circle line), respectively, the triangle line presents the E-field induced H_r shift as a function of the angle. The in-plane direction was defined as 0° and the out-of-plane was defined as 90°.

4 EPR data of reversible test

To verify the stability of the IL gating control of magnetism, out-of-plane H_r shift of Fe_3O_4/MgO heterostructure as a function of ±1.5 V V_g was tested for circles. It is important to obtain normal EPR data for identifying the H_r shift. In Figure S4, the contour map of the out-of-plane FMR spectra for one cycle and 80 cycles were given, showing great tunability and reversibility. Also the four representative EPR data from the first test to the eightieth time were shown, from which we can obtain a stable and reversible EPR signal even after dozens of test.

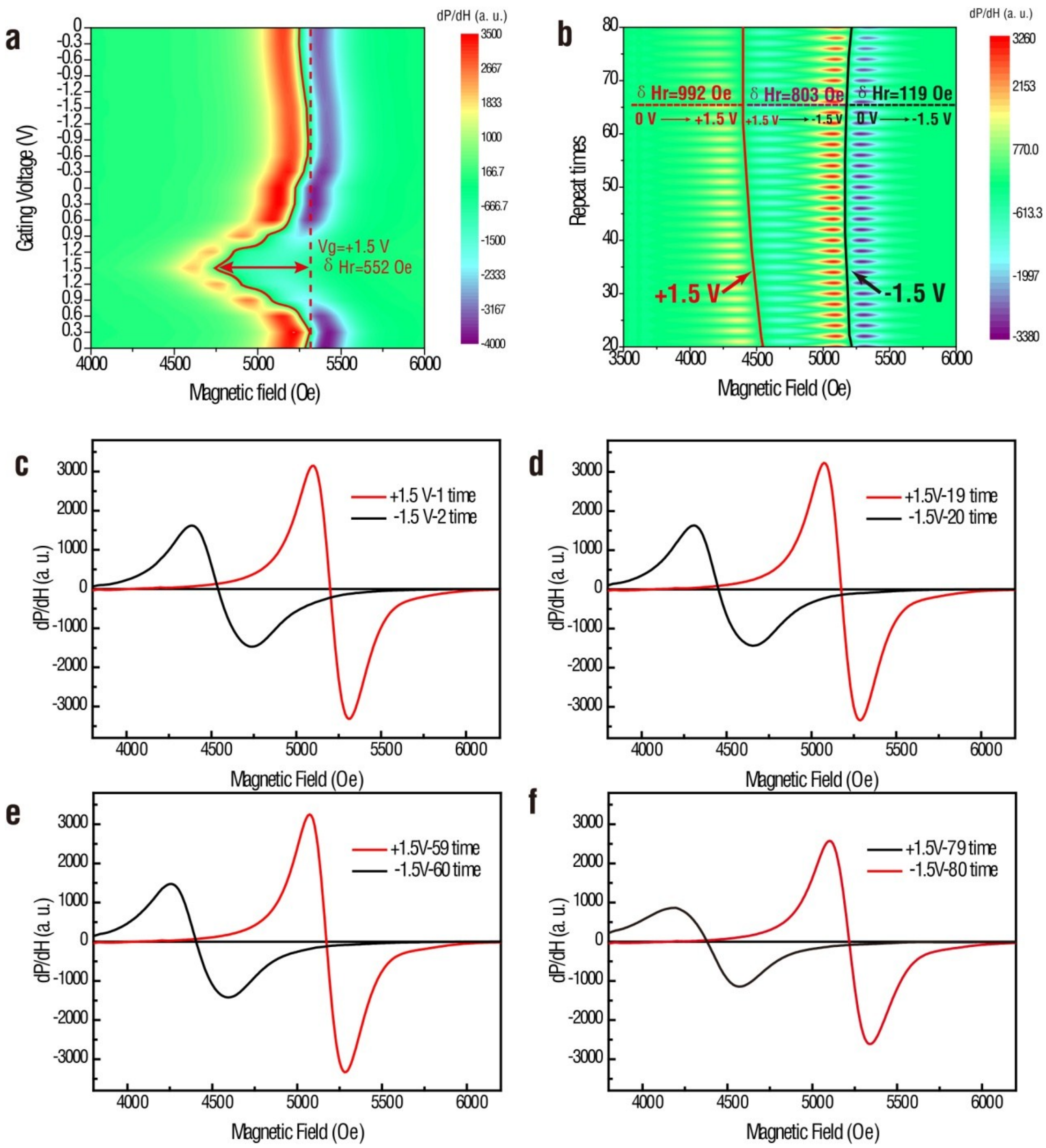

Figure S4a The contour map of the out-of-plane FMR spectra for one cycle. The gating process was the same as that shown in Figure 3(a) in the manuscript. b. the contour map of the out-of-plane FMR spectra for 80 cycles. (c) to (f) the red line and black line represent the H_r at V_g =+1.5 V and -1.5 V, respectively. Figure S3 Representative EPR data of the repeated test

5. Fitting of the measured XRR profile for the ungated, 1.5 V and 5 V gated samples

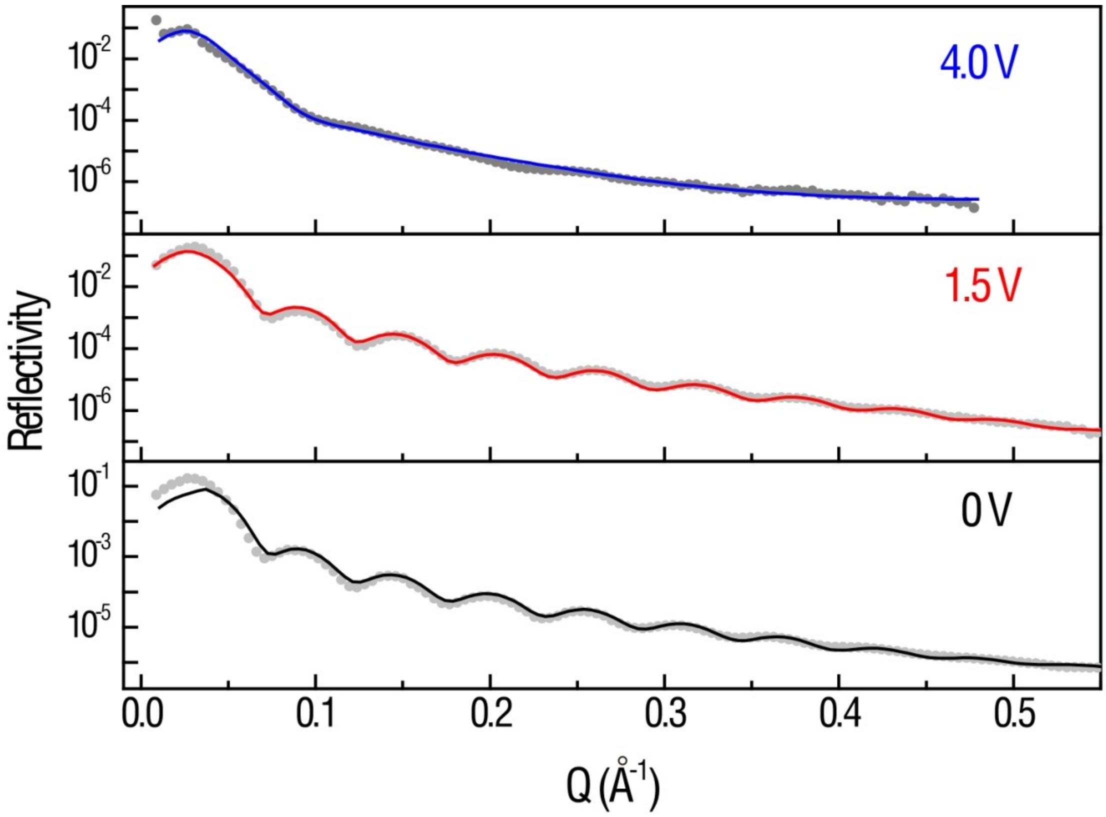

Figure S5 Fitting of the measured XRR profile for different gating voltage

6. EELS data processing

Electron energy loss spectroscopy (EELS) is a powerful technique for this study because the valence state of transition metal Fe can be analyzed by measuring the relative intensity of the transition metal L_3 and L_2 lines. The scan range and line scanning images were shown in Figure S6-1 a-d for ungated and 1.5 V gated Fe_3O_4/MgO heterostructure respectively. In Figure S6e and f, the additional background intensity was removed and L_3 and L_2 values were obtained.

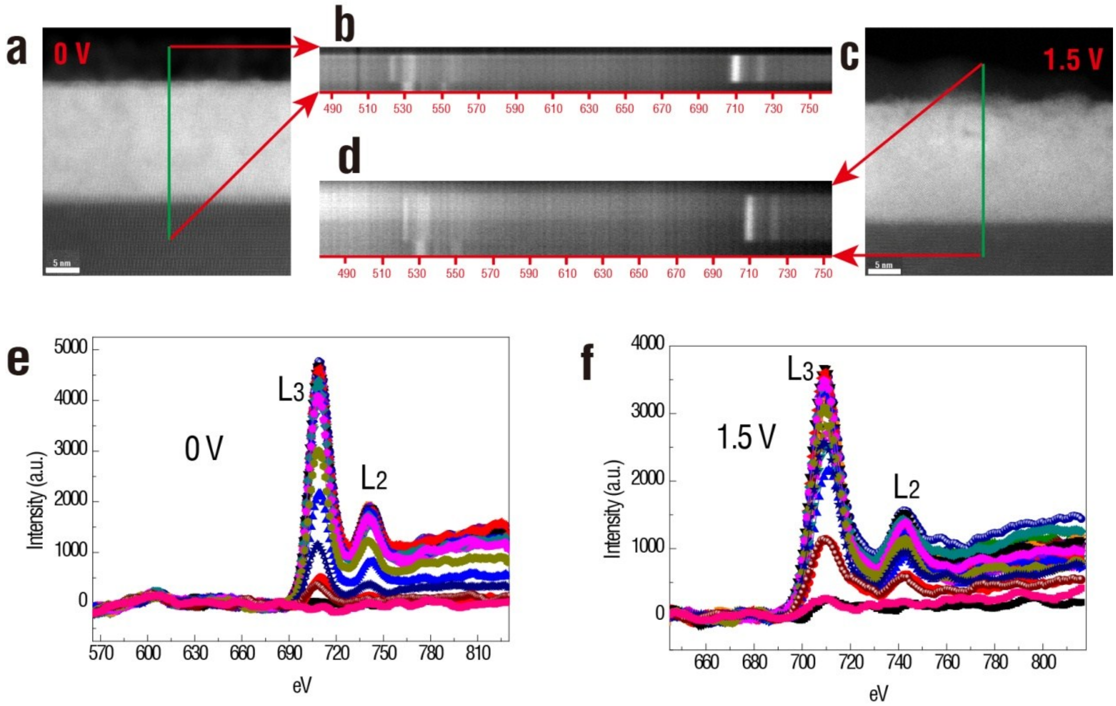

Figure S6-1 (a), (b) and (c), (d) were the scan range and line scanning images for the ungated and 1.5 V gated Fe_3O_4/MgO heterostructure respectively. (e) and (f) shows the L_3 and L_2 intensity with additional background intensity removed.

The L_3/L_2 intensity ratio as a function of the Fe_3O_4 thickness is shown in Figure S6-2 for ungated (blue) and 1.5 V-gated (red) samples. Detailed EELS analysis and data are presented in Figure S6. Within the top 2.5 nm layer of the Fe_3O_4 films, the L_3/L_2 ratio of ungated and 1.5 V-gated samples were very different, indicating a significant drop of Fe^{3+} near the interface during the gating process. In contrast, the L_3/L_2 ratios of both samples are almost identical inside the Fe_3O_4 layer (~17.5 nm), confirming that the IL gating process can only influence the interfacial magnetism of a few nanometers within the chemical window of IL.

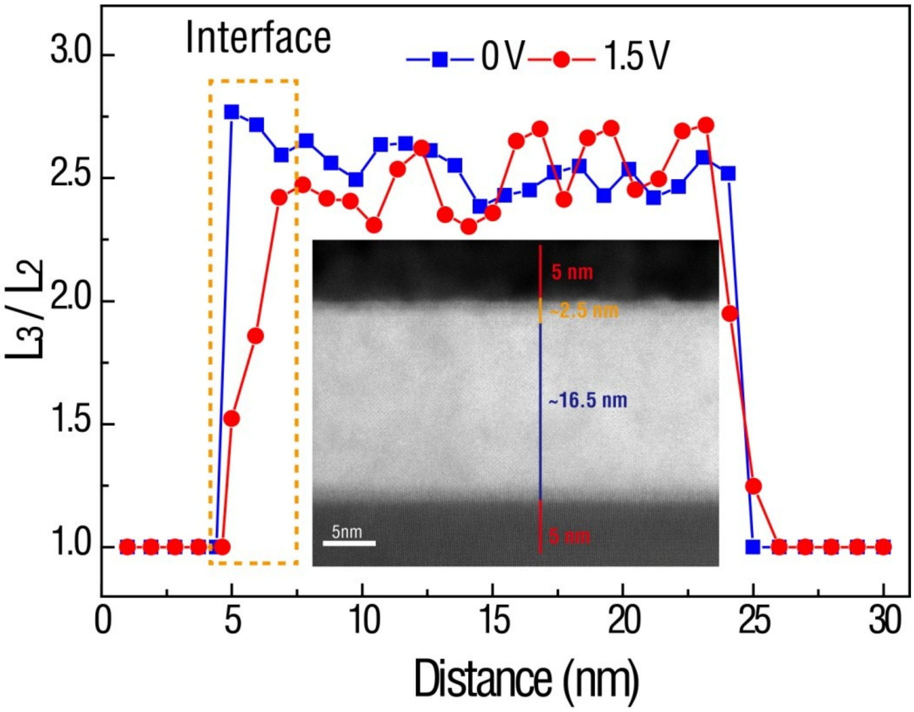

Figure S6-2 L_3/L_2 intensity ratio as a function of the measurement range during the EELS analysis for ungated and +1.5 V-gated samples. The inset displays the EELS analysis range: 5 nm glue, 2.5 nm interface, 16.5 nm Fe_3O_4 layers and 5 nm MgO substrates.

7. The XPS spectra of O 1s of the heterostructures gated at 0 V, 1.5 V and 4 V

The XPS spectra of O 1s of the heterostructures gated at 0 V, 1.5 V and 4 V are shown in Figure S7 a-c. According to the fitting results, the relative content of O bond with Fe (Fe^{2+} and Fe^{3+}) decrease from 32.35%, to 29.96% and then to 24.8% when gating voltage increase from 0 V to 1.5 V and then 4 V. Also we can get the conclusion by the variation of the ratio of Fe^{2+} and Fe^{3+}: during the gating process, parts of Fe^{3+} transfer to Fe^{2+}, to balance the valence, some oxygen should be lost and the oxygen vacancies come out.

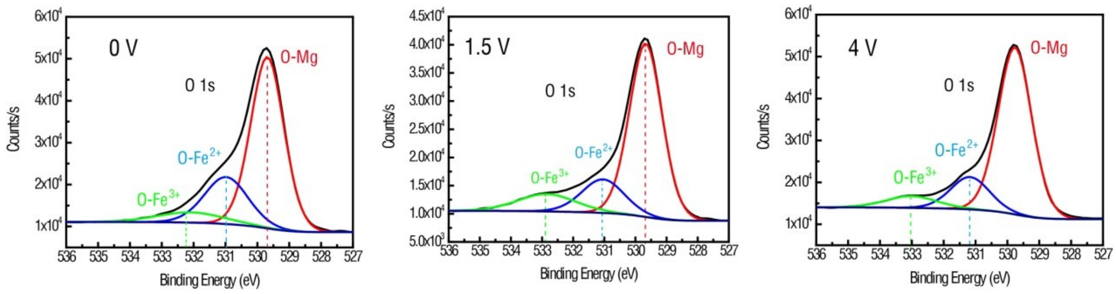

Figure S7 The XPS spectra of O 1s of the heterostructures gated at 0 V, 1.5 V and 4 V

8. Surface morphology for the ungated, 1.5 V and 5 V gated samples

The surface roughness change is negligible for both ungated (0.198 nm) and 1.5 V gated (0.177 nm) due to the extreme bits of chemical reactions. For the Fe_3O_4/MgO heterostructure gated at 5 V in Region II, a drastic roughness increase (0.392 nm) was detected from AFM image in Figure S8(c), which is due to the erosive electrochemical reaction outside the electrochemical window. The existence of destructive chemical reaction here leads to a serious mass loss, significant roughness increasing and an irreversible VCMA.

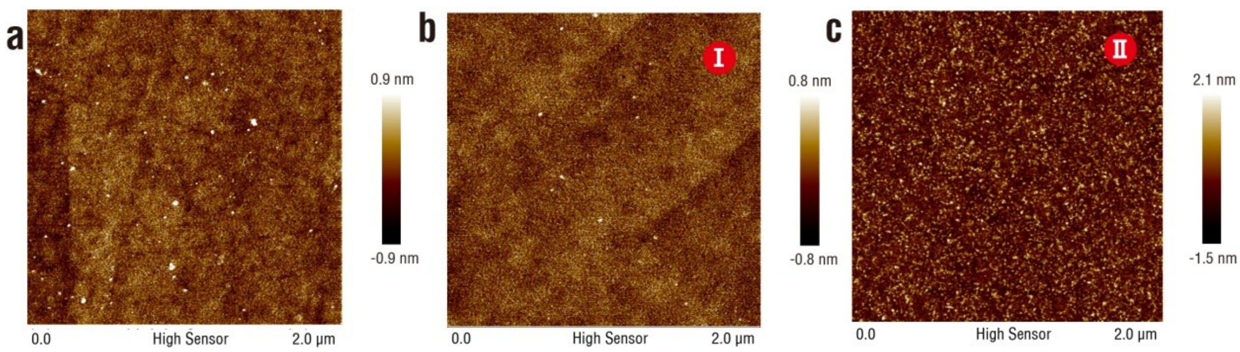

Figure S8 AFM images of ungated, 1.5 V gated and 5 V gated samples